On the MAC for Power-Line Communications: Modeling Assumptions and Performance Tradeoffs

Technical Report

Christina Vlachou*, Albert Banchs†, Julien Herzen*, Patrick Thiran*

*EPFL, Switzerland †Institute IMDEA Networks and University Carlos III of Madrid, Spain

* firstname.lastname@epfl.ch † banchs@it.uc3m.es

Abstract—[1] **Power-line communications are becoming a key component in home networking. The dominant MAC protocol for high data-rate power-line communications, IEEE 1901, employs a CSMA/CA mechanism similar to the backoff process of 802.11. Existing performance evaluation studies of this protocol assume that the backoff processes of the stations are independent (the so-called *decoupling assumption*). However, in contrast to 802.11, 1901 stations can change their state after sensing the medium busy, which introduces strong coupling between the stations and, as a result, makes existing analyses inaccurate.**

In this paper, we propose a new performance model for 1901, which does not rely on the decoupling assumption. We prove that our model admits a unique solution. We confirm the accuracy of our model using both testbed experiments and simulations, and we show that it surpasses current models based on the decoupling assumption. Furthermore, we study the tradeoff between delay and throughput existing with 1901. We show that this protocol can be configured to accommodate different throughput and jitter requirements, and we give systematic guidelines for its configuration.

I. INTRODUCTION

Power-line communications (PLC) are increasingly important in home networking. HomePlug AV, the most popular specification for PLC, is employed by over 120 million devices worldwide [2], and the new HomePlug AV2 devices offer data rates up to 1 Gbps [3]. Moreover, PLC plays a powerful role in hybrid networks comprising wireless, Ethernet, and other technologies [4], as it contributes to increasing the bandwidth of such networks with an independent, widely accessible medium. Yet, despite the wide adoption of HomePlug specifications in home networks, little attention has been paid to providing an accurate analysis and an evaluation of the HomePlug MAC layer.

The vast majority of HomePlug devices employ a multiple-access protocol based on CSMA/CA that is specified by the IEEE 1901 standard[2] [5]. This CSMA/CA mechanism resembles the CSMA/CA mechanism employed by IEEE 802.11, but with important differences in terms of complexity, performance and fairness. The main difference stems from the introduction of a so-called *deferral counter* that triggers a redraw of the backoff counter when a station *senses the*

medium busy. This additional counter significantly increases the state-space required to describe the backoff procedure. Moreover, as we explain in more details later, the use of the deferral counter introduces some level of coupling between the stations, which penalizes the accuracy of models based on the *decoupling assumption*. This assumption was originally proposed in the 802.11 analysis of [6] and has been used in all the works that have analyzed the 1901 CSMA/CA procedure so far (i.e., [7], [8], [9]). In this paper, we show that this decoupling assumption leads to inaccurate results, and the modeling accuracy can be substantially improved by avoiding it.

The decoupling assumption relies on the approximation that the backoff processes of the stations are independent and that, as a consequence, stations experience the same time-invariant collision probability, independently of their own state and of the state of the other stations [6]. In addition, to analyze 1901, it has been assumed that a station senses the medium busy with the same time-invariant probability (equal to the collision probability), during any time slot [7], [8]. In this paper, we show that the deferral counter introduces some coupling among the stations: After a station gains access to the medium, it can retain it for many consecutive transmissions before any other station can transmit. As a result, the collision and busy probabilities are not time-invariant for 1901 networks, which makes the decoupling assumption questionable.

Figures 1 and 2 provide some evidence on the coupling phenomenon described above, for a HomePlug AV testbed with two stations. While Station A transmits during several consecutive slots, Station B is likely to remain in a state where it has a larger probability of colliding or sensing the medium busy. B is then even less likely to attempt a transmission while in this state, and it might have to wait several tens of milliseconds before the situation reverts. Thus, the collision probabilities observed by the stations are clearly time-varying, which invalidates the decoupling assumption. Note that a consequence of this coupling is *short-term unfairness*, which in turn translates into high delay variance (i.e., high jitter).

In this paper, we propose a theoretical framework for modeling the CSMA/CA process of 1901 without relying on the decoupling assumption. First, we introduce a model that accurately captures the 1901 performance without assuming that stations are decoupled. This model is relatively compact: computing the throughput of the network only requires solving

---

[1]This work has been previously published in IEEE ICNP 2014 [1]. This technical report contains additional details and clarifications on the analysis and the proof of Theorem 1 of Section IV.

[2]This CSMA/CA mechanism is the same for all HomePlug specifications, including 1.0, AV, AV2 and GreenPhy.
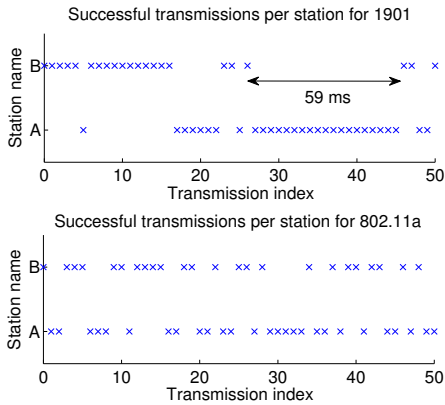
Fig. 1. Testbed trace of 50 successful transmissions by two saturated stations with 1901 and 802.11a. The experimental settings and the details on our testbed are given in Section V-A. 1901 exhibits short-term unfairness: a station holding the channel is likely to keep holding it for many consecutive transmissions (during several tens of ms, for example 59 ms as shown above), which causes high jitter. 802.11 is fairer, which makes the decoupling assumption viable in this case. This experiment took place under ideal channel conditions. In realistic channels, where frames are retransmitted due to errors, the jitter might even be higher.
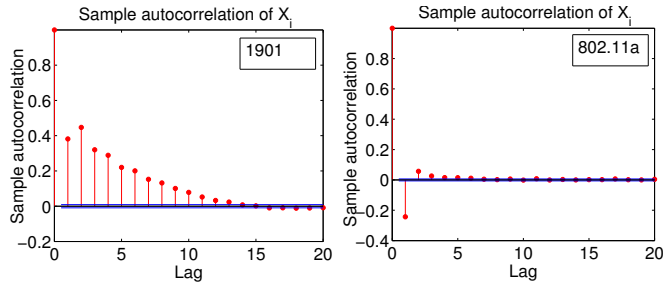

Fig. 2. We study a testbed trace of $5 \cdot 10^4$ successful transmissions for both 1901 and 802.11a when two saturated stations A and B contend for the medium. Let X_i be the variable that indicates which station transmits successfully at the i-th transmission. We take $X_i := 1$ if A transmits and $X_i := 2$ if B transmits. We show the autocorrelation function of X_i, $1 \leq i \leq 5 \cdot 10^4$. Observe that it is positive for 1901 at lags smaller than 15. Hence, if $X_i = 1$ for some i, it is likely that $X_{i+1} = 1$. For 802.11a, we have in contrast a negative value of autocorrelation at lag 1 and a positive one at lag 2, which means that if $X_i = 1$ for some i, it is likely that $X_{i+1} = 2$ and $X_{i+2} = 1$.

a system of m equations, where m is the number of backoff stages (the default value for 1901 is $m = 4$). Second, we prove that this system of equations admits a unique solution. We confirm the accuracy of the model by using both simulations and a testbed of 7 HomePlug AV stations. To the best of our knowledge, this is the first study that validates a 1901 MAC performance model on a real PLC testbed. We have employed a similar testbed setup to study and validate the short-term unfairness (but not a complete model) of the 1901 MAC in [10]. In addition, we investigate the accuracy of our model and that of previous works that rely on the decoupling assumption, showing that, to the best of our knowledge, ours is the first model for 1901 reaching this level of accuracy. Finally, we study in detail the tradeoff between throughput and delay variance (or equivalently, short-term fairness), caused by the deferral counter in 1901. We observe that this tradeoff can be accurately controlled in 1901, and propose a systematic method to configure a 1901 network to obtain the best delay performance under arbitrary throughput constraints.

The remainder of the paper is organized as follows. We present the 1901 backoff process in Section II. We then review the related work on MAC layer in Section III. We present our model for 1901 in Section IV. We evaluate the performance of our model and discuss the decoupling assumption in Section V. We study the tradeoff between throughput and fairness in Section VI. Finally, we give concluding remarks in Section VII.

II. BACKGROUND

In this section, we present the CSMA/CA protocol of 1901 [5], and highlight the mechanism that causes the strong coupling between the stations. This mechanism is the main difference between 1901 and 802.11. In CSMA/CA protocols, such as 802.11, stations wait for a random number of time slots (determined by the *backoff counter*) before transmitting, in the attempt to avoid that some other station transmits at the same slot, which causes a collision. Nevertheless, a collision can still occur and when it does, the stations involved increase the range in which they select their backoff counter (called the *contention window CW*) to further reduce the collision probability. Clearly, there exists a tradeoff: if CW is large, the collision probability is small, but under low-load conditions stations waste many slots on average before transmitting, which decreases throughput. As we explain later, to tackle this backoff inefficiency, 1901 aims at reducing CW. To counterbalance the resulting large collision probability, 1901 introduces an additional mechanism that increases CW *before* a collision occurs: when a station senses a considerable number of transmissions in the channel, it increases CW. To count the number of times a station has to sense the medium busy before increasing CW, a new counter is introduced, called the *deferral counter*.

We now describe the technical details of the 1901 CSMA/CA procedure. It includes three counters: the backoff counter (BC), the deferral counter (DC) and the backoff procedure counter (BPC). Upon the arrival of a new packet, a transmitting station enters backoff stage 0. It then draws the backoff counter BC uniformly at random in $\{0, \ldots, CW_0 - 1\}$, where CW_0 denotes the contention window used at backoff stage 0. Similarly to 802.11, BC is decreased by 1 at each time slot if the station senses the medium to be idle (i.e., below the carrier-sensing threshold), and it is frozen when the medium is sensed busy. In the case the medium is sensed busy, BC is also decreased by 1 once the medium is sensed idle again. When BC reaches 0, the station attempts to transmit the packet. Also similarly to 802.11, the station jumps to the next backoff stage if the transmission fails. In this case, the station increments the BPC counter and enters the next backoff stage. The station then draws BC uniformly at random in $\{0, \ldots, CW_i - 1\}$, where CW_i is the contention window used for backoff stage i, and repeats the process. For 802.11, the contention window is doubled between the successive backoff stages, i.e., $CW_i = 2^i CW_0$. For 1901, CW_i depends on the value of the BPC counter and the priority of the packet: There are four backoff stages that are mapped to the BPC counter, as given in Table I. Also, there are four different priority

Station A

backoff stage i	CW_i	DC	BC
	8	0	3
	⋮	⋮	⋮
	8	0	**0**
	Transmission		
	8	0	7
$i=0$	⋮	⋮	⋮
	8	0	**0**
	Transmission		
	8	0	5
	⋮	⋮	⋮
	8	0	2
$i=1$	16	**1**	6
	⋮		⋮

Station B

backoff stage i	CW_i	DC	BC
	8	0	5
$i=0$	⋮	⋮	⋮
	8	0	2
	16	**1**	11
	⋮	⋮	⋮
	16	1	4
$i=1$			
	16	**0**	3
	⋮	⋮	⋮
	16	0	**0**
	Transmission		
$i=0$	8	0	2
	⋮	⋮	⋮

Fig. 3. An example of the time evolution of the 1901 backoff process with 2 saturated stations A and B. Initially, both stations start at backoff stage 0. Station A wins the channel for two consecutive transmissions. Observe the change in CW_i when a station senses the medium busy and has $DC = 0$. This figure also exposes the short-term unfairness when there are 2 contending stations; a station that grabs the channel for a successful transmission moves to backoff stage 0, whereas the other station enters a higher backoff stage with larger CW and has lower probability to transmit.

classes (CA0 to CA3) that correspond to different values for the CW_i's.

The main difference between 1901 and 802.11 is that a 1901 station might enter the next backoff stage even if it did not attempt a transmission. This is regulated by the deferral counter DC, which works as follows. When the station enters backoff stage i, DC is set at an *an initial DC value* d_i, where d_i is given in Table I for each backoff stage i. After having sensed the medium busy, a station decreases DC by 1 (in addition to BC). If the medium is sensed busy and $DC = 0$, then the station jumps to the next backoff stage (or re-enters the last backoff stage, if it is already at this stage) and re-draws BC, *without attempting a transmission*. An example of such a backoff process is shown in Figure 3.

		Class CA0/CA1		Class CA2/CA3	
backoff stage i	BPC	CW_i	d_i	CW_i	d_i
0	0	8	0	8	0
1	1	16	1	16	1
2	2	32	3	16	3
3	≥ 3	64	15	32	15

TABLE I
IEEE 1901 VALUES FOR THE CONTENTION WINDOWS CW_i AND THE INITIAL VALUES d_i OF DEFERRAL COUNTER DC, FOR EACH BACKOFF STAGE i AND EACH PRIORITY CLASS. CA0/CA1 PRIORITIES ARE USED FOR BEST-EFFORT TRAFFIC AND CA2/CA3 FOR DELAY-SENSITIVE TRAFFIC.

The deferral counter was introduced in 1901, so that 1901 can employ small contention window values – which provide good performance for a small number of stations – while avoiding collisions, thus also providing good performance for a large number of stations[3]. In particular, to reduce collisions, 1901 stations redraw their backoff counter when they sense a number of transmissions before their backoff counter expires; in this way, they can react to a high load in the network without

[3]Indeed, it can be seen from Table I that 1901 contention windows are small.

the need of a collision, which is in contrast to 802.11 that only reacts to collisions.

Although the above mechanism achieves its goal, i.e., providing good performance in terms of throughput, it might lead to short-term unfairness: When a station gets hold of the channel and uses a small contention window, it is likely to transmit several frames and thus trigger the deferral counter mechanism of the other stations, which further increase their contention windows and hence reduce even more their probability of accessing the channel. Such a coupling effect penalizes the accuracy of existing models that assume that the backoff process of different stations are independent. Furthermore, another consequence of this behavior is that a station either holds the channel, and thus experiences low delays, or has to wait a long time before it can transmit. This causes high jitter (i.e., high delay variance).

III. RELATED WORK

The backoff process of 802.11 can be considered as a version of 1901 where the deferral counter DC never reaches 0 (i.e., $d_i = \infty$, for all i). Hence, in the following, we first review relevant studies on 802.11, both with and without the decoupling assumption, and then we present the existing work on 1901. Finally, we discuss related works on fairness.

A. Analyses of IEEE 802.11

Most work modeling 802.11 performance relies on the decoupling assumption, initially proposed by Bianchi in [6]. In his paper, Bianchi proposes a model for single contention domains, using a discrete-time Markov chain to model the backoff procedure of 802.11. Under the decoupling assumption, the collision probability experienced by all stations is time-invariant and can be found via a fixed-point equation that depends on the parameters of the protocol. Kumar et al. [11] examine the backoff process of 802.11 using the same assumptions and renewal theory. The authors also extract a fixed-point equation for the collision probability. Although strong, the decoupling assumption has later been examined and found to be a valid assumption for 802.11 (shown analytically and experimentally in [12], [13], respectively).

Sharma et al. [14] study 802.11 without the decoupling assumption. They analyze an m-dimensional chain (m being the number of backoff stages) that describes the number of stations at each backoff stage. *Drift equations* capture the expected change on the number of stations at each backoff stage between two consecutive time slots, and their equilibrium point yields the average number of stations at each backoff stage in steady state. Similarly to [14], we also use drift equations to obtain an accurate model for 1901, without resorting to the decoupling assumption. However, as the 1901 protocol is much more complex than 802.11, so is our analysis; it differs substantially from the one of [14].

B. Analyses of IEEE 1901 under the Decoupling Assumption

To the best of our knowledge, the only works analyzing the backoff mechanism of 1901 rely on the decoupling assumption.

First, Chung et al. [7] introduce a model using a discrete-time Markov chain similar to Bianchi's model for 802.11 [6]. The additional state required to capture the effect of the deferral counter DC significantly increases the complexity of the Markov chain.

Second, we [8] propose a simplification of the Markov chain [7] and an equivalent model in the form of a single fixed-point equation. We apply the same theoretical framework as [11] and prove that this equation admits a unique solution.

Finally, Cano and Malone [9] provide a simplification of the analysis of [7] for computing the delay under unsaturated traffic scenarios and discuss the assumptions used in [7]. Here too, their analysis relies on the decoupling assumption.

C. MAC Layer Short-Term Fairness

Various investigations evaluating short-term fairness of MAC protocols have been conducted. First, Berger-Sabbatel et al. [15] study the 802.11 short-term fairness both analytically and experimentally. They prove that the 802.11 MAC is short-term fair when there are few contending stations. Second, Bredel and Fidler [16] elaborate more on the 802.11 backoff process and investigate fairness both in short-term and long-term.

Finally, we explore the 1901 fairness both analytically and experimentally using simulation and a testbed in [10]. We reveal that, compared to 802.11, 1901 is short-term unfair, particularly when there are 2 stations contending for the medium.

IV. ANALYSIS

In this section, we introduce our model for the 1901 CSMA/CA procedure. Our analysis relies on the following assumptions:

- There are N stations in the network that belong to a single contention domain.
- All stations are saturated (always have a packet to send).
- There is no packet loss or errors due to the physical layer, and transmission failures are only due to collisions.
- The stations have an infinite retry limit; that is, they never discard a packet until it is successfully transmitted[4].

Furthermore, the 1901 standard specifies that only the stations belonging to the highest contending priority class run the backoff process[5]. In our analysis, we follow this property of 1901, and we consider a scenario in which all the contending stations use the same set of parameters (corresponding to the highest priority class).

Our model is a dynamical system that describes the expected change in the number of stations at each backoff stage between any two consecutive slots. In the stationary regime, the

expected number of stations at each backoff stage is constant, hence we can compute performance metrics by finding the equilibrium of the dynamical system.

Let us now introduce the variables of our model. Let m be the number of backoff stages and let $n_i, 0 \leq i \leq m - 1$ denote the number of stations at backoff stage i. Note that $\sum_{i=0}^{m-1} n_i = N$. Let us further denote with τ_i the transmission probability at stage i, i.e., τ_i is the probability that a station at backoff stage i transmits at any given time slot. In addition, for a given station at backoff stage i, we denote with p_i the probability that at least one other station transmits. We also denote with p_e the probability that no station transmits (or equivalently, that the medium is idle). Under the assumption of independence of the transmission attempts in a single contention domain, we have $p_e = \prod_{k=0}^{m-1} (1 - \tau_k)^{n_k}$, and therefore

$$p_i = 1 - \frac{p_e}{1 - \tau_i} = 1 - \frac{1}{1 - \tau_i} \prod_{k=0}^{m-1} (1 - \tau_k)^{n_k}. \quad (1)$$

In 1901, a station with DC equal to d_i can change its backoff stage either (i) after attempting a transmission or (ii) due to sensing the medium busy $d_i + 1$ times.[6] To compute the probabilities of events (i) and (ii), we introduce x_k^i: it is the probability that a station at backoff stage i jumps to the next backoff stage $i + 1$ in k or fewer time slots due to (ii) (we drop the superscript i in x_k^i when the backoff stage is clear from the context). Note that we can compute x_k^i directly from p_i. Let T be the random variable describing the number of slots among k slots during which the medium is sensed busy. Because a station at backoff stage i senses the medium busy with probability p_i at each time slot, T follows the binomial distribution $\mathrm{Bin}(k, p_i)$. This yields

$$x_k^i = \mathbb{P}(T > d_i) = \sum_{j=d_i+1}^{k} \binom{k}{j} p_i^j (1 - p_i)^{k-j}. \quad (2)$$

Let us denote with bc_i the expected number of time slots spent by a station at backoff stage i. Now, recall that when entering stage i, the stations draw a backoff counter BC uniformly at random in $\{0, \ldots, CW_i - 1\}$. Let k denote the value of BC, and d_i be the value of DC when the station enters stage i. Depending on k, one of the following happens:

- If $k > d_i$, then event (i) occurs with probability $(1 - x_k^i)$, in which case the station spends $(k + 1)$ slots in stage i (the $(k+1)th$ slot being used for transmission). This event is illustrated by the two transmissions of station A in Figure 3. Now, (ii) occurs with probability x_k^i. More precisely, (ii) occurs at slot j, for $d_i + 1 \leq j \leq k$, with

---

[4]Contrary to 802.11, the 1901 standard does not specify a retry limit. There is a timeout on the frame transmission which is vendor specific. For instance, for the HomePlug AV devices, the timeout for CA1 priority frames is 2.5 s, which is very large compared to the maximum frame duration (2.5 ms [5]). Therefore, this hypothesis is not strong.

[5]In practice, the contending priority class is decided during a so-called *priority resolution phase*, using a simple system of busy tones.

[6]A major difference between 1901 and 802.11 is that, contrary to 1901, a station using 802.11 can only adapt its backoff because of (i), not of (ii).

probability $(x_j^i - x_{j-1}^i)$[7], in which case the station spends j slots in stage i.

- If $k \le d_i$, then (ii) cannot happen. Event (i) takes place with probability 1, which yields that the backoff counter expires and that the station spends $(k+1)$ slots in stage i.

By grouping all the possible cases described above, it follows that bc_i is given by

$$bc_i = \frac{1}{CW_i} \sum_{k=d_i+1}^{CW_i-1} \left[(k+1)(1-x_k) + \sum_{j=d_i+1}^{k} j(x_j - x_{j-1}) \right] + \frac{(d_i+1)(d_i+2)}{2CW_i}. \qquad (3)$$

Now, the transmission probability τ_i can be expressed as a function of x_k^i and bc_i, using the renewal-reward theorem, with the number of backoff slots spent in stage i being the renewal sequence and the number of transmission attempts (i.e., 0 or 1) being the reward. The expected number of transmission attempts at stage i can be computed similarly to bc_i. Hence, by dividing the expected transmission attempts at stage i with the expected time slots spent at stage i, τ_i is given by

$$\tau_i = \frac{\sum_{k=d_i+1}^{CW_i-1} \frac{1}{CW_i}(1-x_k) + \frac{d_i+1}{CW_i}}{bc_i}. \qquad (4)$$

Similarly, we define β_i as the probability that, at any given slot, a station at stage i moves to the next backoff stage because it has sensed the medium busy $d_i + 1$ times. It can be easily seen that β_i is given by

$$\beta_i = \frac{\sum_{k=d_i+1}^{CW_i-1} \frac{1}{CW_i} \sum_{j=d_i+1}^{k} (x_j - x_{j-1})}{bc_i}. \qquad (5)$$

Note that τ_i and β_i are functions of p_i (through x_k^i and bc_i).

Notation	Definition (at backoff stage i, $0 \le i \le m-1$)
n_i	Number of stations
$\bar{n}_i$	Expected number of stations
p_i	Probability that at least one other station transmits at any slot
p_e	Probability that the medium is idle at any slot (same for all i)
x_k^i	Probability that a station leaves stage i due to sensing the medium busy $d_i + 1$ times (the backoff counter does not expire)
bc_i	Expected number of backoff slots
τ_i	Probability that a station transmits at any slot
β_i	Probability that a station leaves stage i due to sensing the medium busy $d_i + 1$ times at any slot
F_i	Expected change in n_i between two consecutive slots

TABLE II
NOTATION LIST

[7]Observe that $(x_j^i - x_{j-1}^i)$ is the difference of two complementary CDFs and denotes the probability that (ii) happens exactly at slot j. The probability that a station jumps to the next backoff stage exactly at slot j is $\binom{j-1}{d_i} p_i^{d_i+1}(1-p_i)^{j-d_i-1}$, because the station senses the medium busy for d_i times in any of the $j-1$ slots, and for the $(d_i+1)th$ time at the jth slot. As x_j^i is a complementary CDF of a binomial distribution, we can express it as an incomplete beta function $x_j^i = 1 - I_{1-p_i}(j - d_i, d_i + 1)$ [17]. Now, by the property $I_z(a+1, b) = I_z(a, b) - (\Gamma(a+b)/(\Gamma(a)\Gamma(b)))(1-z)^b z^a$ of the incomplete beta function [18] with $z = 1 - p_i$, $a = j - d_i - 1$, $b = d_i + 1$ and $\Gamma(n) = (n-1)!$, it can be seen that indeed $(x_j^i - x_{j-1}^i) = \binom{j-1}{d_i} p_i^{d_i+1}(1-p_i)^{j-d_i-1}$.

We next introduce our model. A key feature of our model is that we do not assume that the stations are decoupled, as the collision probability is allowed to depend on the station's state. To study the system, we use a vector that includes the number of stations at each backoff stage. In particular, let $X(t) = (X_0(t), X_1(t), \ldots, X_{m-1}(t))$ represent the number of stations at each backoff stage $(0, 1, \ldots, m-1)$ at time slot t. We use the notation $n(t) = (n_0(t), n_1(t), \ldots, n_{m-1}(t))$ to denote a realization of $X(t)$ at some time slot t.

To analyze our system, we assume that the backoff counters are geometrically distributed with the same mean of that of the real uniform distribution. With this assumption, a station at backoff stage i transmits at any slot t with a constant probability τ_i given by (4), independently from the previous slots, and the vector $X(t)$ is a Markov chain. Furthermore, we assume that at backoff stage i a station might move to the next backoff stage due to sensing the medium busy with probability β_i. Note that p_i, τ_i, and β_i can be computed from (1), (4) and (5), given the state vector $n(t)$ (hereafter, to simplify notation we drop the input variable t from $p_i(t)$, $\tau_i(t)$, $\beta_i(t)$, and $n(t)$ as the equations are expressed for any slot t).

Let now $F(n) = \mathbb{E}[X(t+1) - X(t)|X(t) = n]$ be the expected change in $X(t)$ over one time slot, given that the system is at state n. The function $F(\cdot)$ is called the *drift* of the system, and is given by

$$F_i(n) = \qquad\qquad\qquad\qquad\qquad (\text{DRIFT})$$
$$\begin{cases} \sum_{k=0}^{m-1} n_k \tau_k (1-p_k) - n_0(\tau_0 + \beta_0), & i = 0 \\ n_{i-1}(\tau_{i-1}p_{i-1} + \beta_{i-1}) - n_i(\tau_i + \beta_i), & 0 < i < m-1 \\ n_{m-2}(\tau_{m-2}p_{m-2} + \beta_{m-2}) - n_{m-1}\tau_{m-1}(1-p_{m-1}), & \\ \qquad\qquad\qquad\qquad\qquad\qquad i = m-1. \end{cases}$$

(DRIFT) is obtained by balancing, for every backoff stage, the average rate of stations that enter and leave this backoff stage. In particular, F_0 increases only when some stations transmit successfully. Since such stations could be in any of the other backoff stages and there are n_k stations in stage k, this occurs at rate $\sum_{k=1}^{m-1} n_k \tau_k (1 - p_k)$. Similarly, F_0 decreases when some stations at stage 0 are either involved in a collision (which occurs with probability $n_0 \tau_0 p_0$), or do not transmit and sense the medium busy $d_0 + 1$ times (which occurs with probability $n_0 \beta_0$). The decrease of the drift in both cases is 1, thus the expected decrease is equal to the sum of the two probabilities.

Similarly, F_i, $0 < i < m-1$ is computed by observing that in these backoff stages, F_i changes if and only if some stations sense the medium busy, or transmit. Finally, F_{m-1} increases after some stations at stage $m-2$ experience a collision or sense the medium busy $d_{m-2}+1$ times. It decreases only after a successful transmission at stage $m-1$.

The evolution of the expected number of stations $\bar{n}(t) := \mathbb{E}[X(t)]$ is described by the m-dimensional dynamical system

$$\bar{n}(t+1) = \bar{n}(t) + F(\bar{n}(t)), \qquad (6)$$

where $F(\bar{n}(t))$ is given by (DRIFT). In order to know the average number of stations at each backoff stage at steady state,

we can compute the equilibrium point(s) of this system, which is the stationary regime where the average number of stations at each backoff stage remains constant. This information will later enable us to compute actual throughput figures.

Next, we compute the equilibrium point of (6) by imposing $F(\bar{n}(t)) = 0$, which yields

$$\bar{n}_i = \left(\frac{\tau_{i-1}p_{i-1} + \beta_{i-1}}{\tau_i + \beta_i} \right) \bar{n}_{i-1}, \quad 1 \le i \le m-2,$$

$$\bar{n}_{m-1} = \left(\frac{\tau_{m-2}p_{m-2} + \beta_{m-2}}{\tau_{m-1}(1 - p_{m-1})} \right) \bar{n}_{m-2}.$$

Let us define

$$K_0 := 1, \; K_i := \frac{\tau_{i-1}p_{i-1} + \beta_{i-1}}{\tau_i + \beta_i}, \quad 1 \le i \le m-2,$$

$$K_{m-1} := \frac{\tau_{m-2}p_{m-2} + \beta_{m-2}}{\tau_{m-1}(1 - p_{m-1})}. \tag{7}$$

Since $\sum_{i=0}^{m-1} \bar{n}_i = N$, it follows that the equilibrium of system (6) is given by the following system of equations:

$$\bar{n}_0 = \frac{N}{\sum_{k=0}^{m-1} \prod_{j=0}^{k} K_j}, \bar{n}_i = \frac{N \prod_{j=0}^{i} K_j}{\sum_{k=0}^{m-1} \prod_{j=0}^{k} K_j} \; 1 \le i \le m-1. \tag{EQ}$$

Recall that τ_i and β_i are functions of p_i, given by (4) and (5). Thus, the $\bar{n}_i$'s in (EQ) are also functions of p_i, $0 \le i \le m-1$. From the above, substituting (EQ) in (1) yields a system of m equations and m unknowns p_i for $0 \le i \le m-1$. The following theorem is one of our main results. It states that, for configurations satisfying $CW_{i+1} \ge 2CW_i - d_i - 1$, $0 \le i < m-1$, the system (EQ), (1) admits exactly one solution, hence that the equilibrium point of (6) is unique. Note that, from Table I, these constraints are compliant with the standard, except for the class CA2/CA3 at backoff stage $i = 1$. We leave the extension of the uniqueness result to this priority class, and the investigation of the stability of (6) for future work.

Theorem 1. *Assume that $CW_i \ge 6$ and $d_i \le \lfloor CW_i/2 - 1 \rfloor$, $0 \le i \le m-1$. In addition, assume that $CW_{i+1} \ge 2CW_i - d_i - 1$, $0 \le i < m-1$. Then the system of equations formed by (EQ) has a unique solution.*

Proof: Recall that $p_e = \prod_{k=0}^{m-1} (1 - \tau_k)^{\bar{n}_k}$. Combining (1) with (4) and given Proposition 2 in Appendix, τ_i can be computed as a function of p_e, and so can β_i, p_i. Hence, $\bar{n}_i$ can also be computed as a function of p_e, given (EQ). With this, let $\Phi(p_e) := \prod_{k=0}^{m-1} (1 - \tau_k(p_e))^{\bar{n}_k(p_e)}$. Then, a solution of (EQ) has to satisfy the following equation:

$$p_e = \Phi(p_e). \tag{8}$$

We first show that there exists at least one value of p_e that satisfies (8). Observe that our system of equations has as unknowns the p_i's, and that we have $0 \le p_i \le 1, 1 \le i \le m-1$. Let $\tau_0^{max} := 2/(CW_0 + 1)$ denote the maximum transmission probability at stage 0. Then, p_e is defined in $[0, 1 - \tau_0^{max}]$, according to Proposition 1 in Appendix. Because we have $n_i \ge 0$ and $\tau_i < 1$ (the maximum value of τ_i is $2/(CW_i + 1)$

according to Lemma 1), at $p_e = 0$ we obtain $\Phi(0) > 0$. Now, by computing $\Phi(1 - \tau_0^{max})$, it is easy to see that the result is $\Phi(1 - \tau_0^{max}) = (1 - \tau_0^{max})^N < 1 - \tau_0^{max}$ (we only study the case $N > 1$, since for $N = 1$ the solution to the model is trivial). Therefore, by the intermediate value theorem, $\Phi(p_e)$ has at least one fixed-point in $[0, 1 - \tau_0^{max}]$.

We next show that there exists only one value of p_e that satisfies (8). To this end, we show that $\Phi(p_e)$ is monotonically decreasing with p_e. The derivative of $\Phi(p_e)$ can be written as

$$\frac{d\Phi(p_e)}{dp_e} = \sum_{j=0}^{m-1} \left(\frac{\partial\Phi}{\partial p_j} \frac{dp_j}{dp_e} + \frac{\partial\Phi}{\partial\beta_j} \frac{d\beta_j}{dp_e} + \frac{\partial\Phi}{\partial\tau_j} \frac{d\tau_j}{dp_e} \right). \tag{9}$$

We now examine separately each of the partial derivative products of (9) with respect to p_j, β_j and τ_j.

First, by Lemma 4 in Appendix, $\partial\Phi/\partial p_j > 0$. Since $dp_j/dp_e = (dp_j/d\tau_j) \cdot (d\tau_j/dp_e)$, it follows from Lemmas 1 and 2 in Appendix that $dp_j/dp_e < 0$. Thus, the first product of partial derivatives in (9) is negative for all j. Second, by Lemma 3 in Appendix, $\partial\Phi/\partial\beta_j \ge 0$. Moreover, Corollary 2 states that $d\beta_j/dp_j > 0$ and we have shown above that $dp_j/dp_e < 0$. Hence, we have $d\beta_j/dp_e < 0$, and the second product of partial derivatives in (9) is also negative. Finally, it follows from Lemma 5 that $\partial\Phi/\partial\tau_j < 0$, and by Lemma 2 we have $d\tau_j/dp_e > 0$. We have shown that all the partial derivative products of (9) are negative hence, $\Phi(p_e)$ monotonically decreases with p_e.

Since (9) is strictly negative, there exists a unique value for $p_e \in [0, 1 - \tau_0^{max}]$ that solves (8). Computing the corresponding value for p_i by (1), we have a solution to (EQ). The uniqueness of the solution then follows from the fact that all relationships between τ_i, β_i, p_i and p_e are bijective, and any solution must satisfy (8), which (as we have shown) has only one solution. ∎

Figure 4 illustrates that the average number of stations at each state obtained from simulations stays close to the deterministic trajectory of the dynamical system (6) at all times, and that indeed, the system converges to the equilibrium point. We plan to investigate the stability of the equilibrium
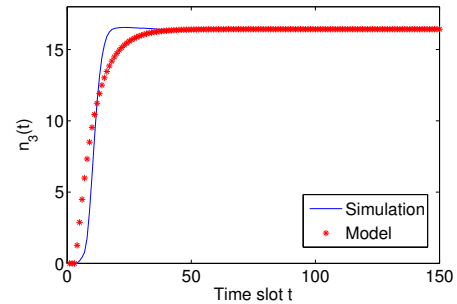

Fig. 4. Expected number of stations at backoff stage 3 computed with our model, and also computed via 5,000 simulations, for a network with 20 stations using the default CA1 configuration of 1901 $\bar{n}_3(t)$ is shown as a function of the time slot t, with initial condition $\bar{n}_0(0) = 20$ and $\bar{n}_i(0) = 0$, $0 < i \le 3$.

point (EQ) in our future work.

In Section V, we observe that our model is very accurate for all configurations. We explain how collision probability and throughput are computed in the same section.

V. Performance Evaluation

In this section, we evaluate the 1901 performance under different configurations. First, we validate experimentally our simulator and our model by using a testbed. Second, we evaluate our model and compare it with the models based on the decoupling assumption [7], [8]. These models perform different computations, but are strictly equivalent in terms of predicted throughput. We thus refer to these models as (the unique) "D.A." model.

A. Experimental Validation

We use simulations to evaluate 1901 performance. We wrote a Matlab simulator, which implements the full CSMA/CA mechanism of 1901[8]. In this subsection, we validate the accuracy of our model and simulator with experimental results from a HomePlug AV test-bed.

We built a test-bed of 7 stations, each comprising a PLC interface[9]. The stations are ALIX boards running the OpenWrt Linux distribution [20]. Each board is equipped with a Home-plug AV miniPCI card (Intellon INT6300 chip). In our tests, N stations send UDP traffic (at a rate higher than the link capacities) to the same non-transmitting station using *iperf*. We run tests for $1 \leq N \leq 6$. At the end of each test we request the number of collided and successfully transmitted frames from each station using the *Qualcomm Atheros Open Powerline Toolkit* [21]. Using this information, we evaluate the collision probability.

We compare the collision probability measured on the testbed with the one obtained with our model. To this end, we use our model to compute the steady-state expected number of nodes $\bar{n}_0, \ldots, \bar{n}_{m-1}$ at each backoff stage. Once we have the average number of stations at each each backoff stage, the probability p_i of collision at backoff stage i is readily given by (1).

Let γ be the average probability that a transmission in the system collides. The probability that a given transmission in the system corresponds to a station at backoff stage i is given by $\bar{n}_i \tau_i / \sum_{k=0}^{m-1} \bar{n}_k \tau_k$. We thus have $\gamma = \sum_{i=0}^{m-1} \bar{n}_i \tau_i p_i / \sum_{i=0}^{m-1} \bar{n}_i \tau_i$.

The average collision probabilities obtained from 10 testbed experiments, 10 simulation runs, and our model are shown in Figure 5. We observe an excellent fit between experimental and simulation/analytic results.

Contrary to some existing 802.11 interfaces, the MAC parameters of the HomePlug AV devices cannot be modified,
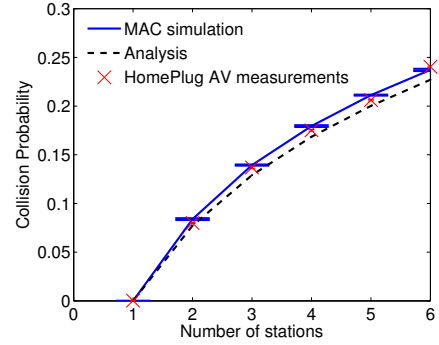

Fig. 5. Collision probability obtained by simulation, our drift model of Section IV and experiments with HomePlug AV devices for the default configuration CA1 of 1901 given in Table I.

because they are stored in the firmware, and the required off-sets of their binary values are not publicly available. Therefore, the results on throughput and fairness have been obtained with our validated simulator.

B. Simulation Parameters and Throughput Computation

Our simulator uses the same time slot duration and timing parameters as specified in the standard (see Table III). The PLC frame transmission has a duration D and is preceded by two priority tone slots (PRS), and a preamble (P). It is followed by a response inter-frame space ($RIFS$), the ACK, and finally, the contention inter-frame space ($CIFS$). Thus, a successful transmission has a duration $T_s := 2PRS + P + D + RIFS + ACK + CIFS$. In the case of a collision, the stations set the virtual carrier sense (VCS) timer equal to $EIFS$, where $EIFS$ is the extended inter-frame space used by 1901, and then the channel state is *idle*. Hence, a collision has a duration $T_c := EIFS$. Finally, we assume that all the packets use the same physical rate.

Parameter	Duration (μs)
Slot σ, Priority slot PRS	35.84
$CIFS$, $RIFS$	100.00
Preamble P, ACK	110.48
Frame duration D	2050.00
$EIFS$	2920.64

TABLE III
SIMULATION PARAMETERS.

To analytically evaluate throughput, we employ the model of Section IV. After solving the equations for finding the steady-state number of nodes $\bar{n}_0, \ldots, \bar{n}_{m-1}$ at each backoff stage, we can compute the throughput of the network as follows. The probability that a slot is idle is p_e. The probability of a successful transmission of a station at stage i is $\tau_i(1 - p_i)$. Therefore, the probability p_s that a slot contains a successful transmission is given by $p_s = \sum_{i=0}^{m-1} \bar{n}_i \tau_i(1 - p_i)$. Let p_c denote the probability that a slot contains a collision. We have $p_c = 1 - p_e - p_s$. We now have enough information to compute the normalized throughput S of the network as

$$S = \frac{p_s D}{p_s T_s + p_c T_c + p_e \sigma}, \tag{10}$$

---

[8]Our simulator and the guidelines to reproduce all the testbed experiments of this work are available in [19].

[9]The stations also have a wireless interface, a miniPCI card Atheros DNMA-92. This interface is used only for the experiments of Section I. To avoid interference with other devices in our building we set the mode to 802.11a and the wireless channel to 44. To obtain the packet trace of Figures 1, 2 for 802.11a we use `tcpdump`. To capture the transmitted frames for 1901, we use the tools described in [19], because this MAC employs frame aggregation and the number of Ethernet packets per PLC frame varies with time.
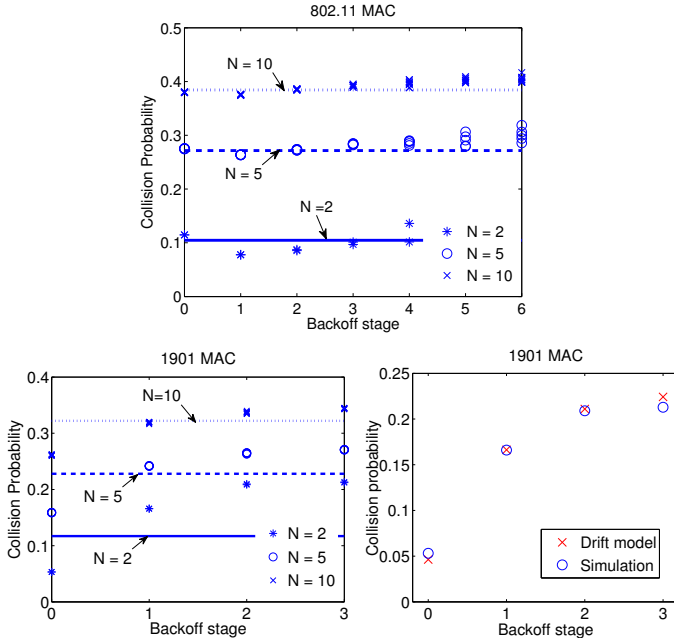
Fig. 6. Simulations of 1901 (with CA1 parameters) and 802.11 for $N = 2, 5, 10$. Points show the collision probabilities at different backoff stages for all stations, and lines represent the solution of the fixed-point equations for the collision probability from the D.A. models [6], [8]. The decoupling assumption is viable for 802.11 even for $N = 2$, whereas the collision probability depends on the backoff stage for 1901. Our model accurately predicts the collision probability at each backoff stage i (shown at the right for $N = 2$).

where D is the frame duration, T_s is the duration of a successful transmission, T_c is the duration of a collision, and σ is the time slot duration.

C. The Decoupling Assumption Does Not Hold for 1901

For 802.11, the decoupling assumption has been shown to be viable in various settings as $N \to \infty$ [12]. In addition, it turns out that it also works well for small numbers of stations [6], [13]. For 1901, the coupling induced by the deferral counter makes the collision probabilities state-dependent, which penalizes models based on the decoupling assumption when N is small. To see this, we plot on Figure 6 the collision probabilities experienced by 802.11 and 1901 stations, as a function of the backoff stage (i.e., as a function of the stations' state). On the same figure, we also show the collision probabilities computed with our model. Let C_k be the sequence of outcomes of attempted transmissions, i.e. $C_k := 0$ if the kth transmission attempt results in a success, and $C_k := 1$ when the outcome is a collision. The decoupling assumption asserts that the sequence $\{C_k\}$ consists of independent and identically distributed (i.i.d.) random variables. In Figure 6, we observe that for 1901, $\{C_k\}$ cannot be considered as i.i.d., because the collision probability observed at different backoff stages is not the same. The collision probability depends on the previous transmission attempts (backoff stage changed due to collision) or on other stations activity (backoff stage changed due to sensing the medium busy). In fact, the collision probability for 1901 is an increasing sequence of the backoff stage i, as shown in Figure 6, and proved in Corollary 1 in Appendix.

D. Model Evaluation

We now compare our drift model with the D.A. model for various configurations and number of stations. In Figure 7, we show the throughput obtained by 1901 with the default parameters for the two priority classes CA1 and CA3 (CA0 and CA2 are equivalent). We also show the throughput predicted by the two models. The model based on the decoupling assumption is less accurate for CA1 when N is small, because the class CA1 uses larger contention windows, which increases the time spent in backoff and, as a result, the coupling between stations.
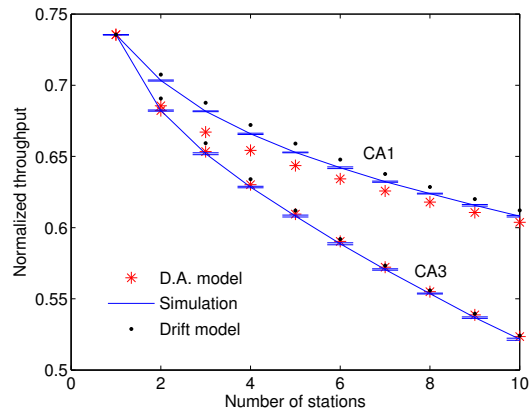

Fig. 7. Throughput obtained by simulation, with our model, and the models based on the decoupling assumption (D.A.), for the default configurations of 1901 given in Table I.

We now study the accuracy of the two models in more general settings. To this end, we introduce a factor f, such that at each stage i, the value of d_i is given by $d_i = f^i(d_0 + 1) - 1$. This enables us to define various sequences of values for the d_i's, using only f and d_0. At each stage i, CW_i is given by $CW_i = 2^i CW_{min}$, and there are m backoff stages ($i \in \{0, m-1\}$). In Figure 8, we show the throughput for various such values of d_0 and f, with $CW_{min} = 8$ and $m = 4$. We observe that the D.A. model achieves good accuracy when the d_i's are large, because in these configurations, the deferral counter is less likely to expire, which reduces the coupling among stations. Note that the drift model achieves good accuracy when the d_i's are small.
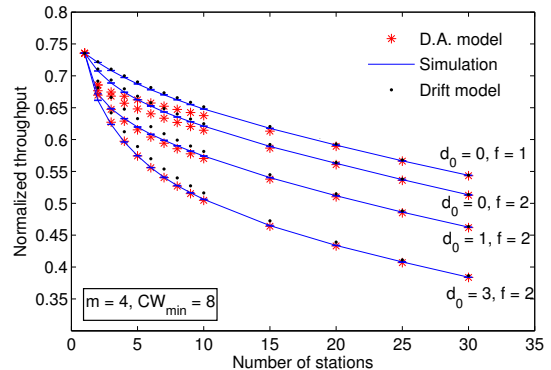

Fig. 8. Throughput obtained by simulation, with the drift model, and the D.A. model for different configurations. The initial values d_i of the deferral counter at each backoff stage are given by $d_i = f^i(d_0 + 1) - 1$.

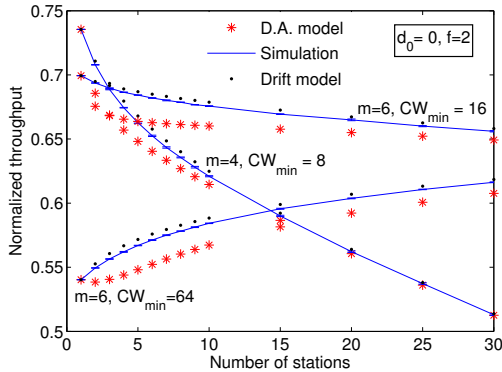Finally, in Figure 9 we show the throughput for different

Fig. 9. Throughput obtained by simulation, with the drift model, and the D.A. model for various values of CW_{min} and $m \in \{4,6\}$.

values for CW_{min}, with $m \in \{4,6\}$. In all cases, the drift model fits very well, contrary to the model based on the decoupling assumption. The accuracy of the D.A. model is penalized more when CW_{min} is large, because the likelihood that the deferral counter expires increases.

VI. THROUGHPUT, FAIRNESS AND COUPLING

In this section we show how the coupling between 1901 stations is related to throughput and jitter (or, equivalently, unfairness). Moreover, based on our model, we propose a method to optimize jitter under a given throughput requirement.

In the introductory example of Figure 1, we observe a bistability effect with two 1901 stations, where stations are likely to remain for long durations in states with large transmit (resp. backoff) probabilities. We explain that this effect is caused by the deferral counter, which creates a coupling between the stations and penalizes the accuracy of models assuming decoupling. It turns out that this coupling is beneficial for throughput[10], and different 1901 configurations determine different tradeoffs between fairness (or jitter) and throughput. We now investigate this effect further in terms of short-term fairness. A MAC protocol is short-term fair when the stations get similar transmission opportunities over short time scales. Conversely, an unfair protocol advantages some stations over others, which in practice results in high delay variance (jitter). To measure short-term fairness, we compute Jain's fairness index [22] over windows of N frame durations. More precisely, if we let $x_i(w)$ be the number of frames successfully transmitted by station i during a window of w frame durations, Jain's index during window w is defined as $J(w) = (\sum_{i=1}^{N} x_i(w))^2 / (N \sum_{i=1}^{N} x_i(w)^2)$. In the following, we take $w = N$, as this is the smallest value of w such that $J(w)$ can be equal to 1 (for a perfectly fair protocol). The reported results are obtained by averaging the values of $J(N)$ over windows moving along the whole packet traces.

In Figure 10, we plot throughput and short-term fairness as a function of the initial values of the deferral counter (in terms of d_0 and f), for $N = 2$ and $N = 5$. Interestingly, it appears that that there is a direct link between throughput,

[10]Intuitively, this is easy to understand: without proper synchronization, having one station transmitting for long durations is more efficient than alternating transmissions.
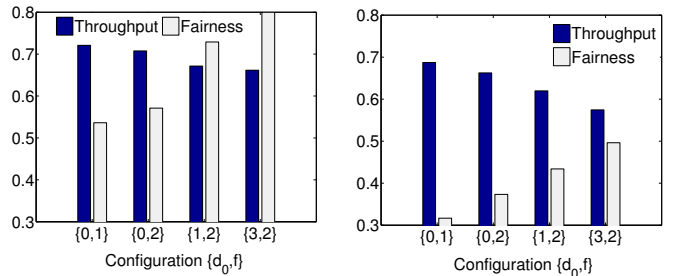

Fig. 10. Throughput and fairness with $CW_{min} = 8$ and $m = 4$ and various values of d_0 and f, for $N = 2$ (left) and $N = 5$ (right). The initial value of the deferral counter at backoff stage i is given by $d_i = f^i(d_0 + 1) - 1$.
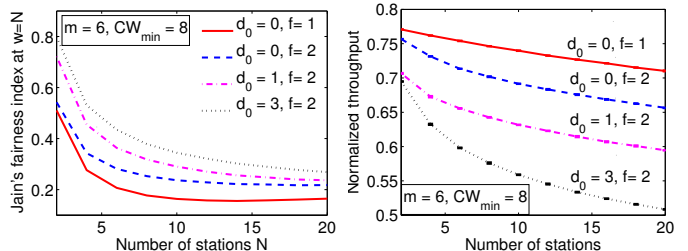

Fig. 11. Short-term fairness and throughput obtained by simulation for parameters $CW_{min} = 8$, $m = 6$ and various values of d_0 and f. The deferral counter tunes a tradeoff between throughput and fairness in 1901.

fairness and coupling. When the initial deferral counters are small (corresponding to small d_0 and f), the stations are more likely to react on sensing the medium busy and thus become coupled. Indeed, as confirmed by Figure 8, the configurations employing small deferral counters yield larger throughput but lower accuracy when assuming decoupling. Conversely, these configurations have the worse short-term fairness and thus cause higher jitter.

We study further the throughput/fairness tradeoff on Figures 11 and 12. Both figures show the throughput and fairness achieved on networks with a varying number of stations. Figure 11 presents throughput and fairness for various initial deferral counter values (in terms of d_0 and f). Figure 12 shows these two metrics for different numbers of backoff stages m.

Again, both figures show a clear tradeoff between throughput and short-term fairness. Furthermore, this tradeoff can be tuned by adapting the parameters that control the number of backoff stages and the initial values of the deferral counters. This possibility is a remarkable feature of 1901, enabled by the deferral counter. We summarize the impact of all parameters on throughput and fairness in Table IV.

A. Finding Efficient Configurations

We can use the findings summarized in Table IV, together with our drift model, to find efficient configurations that meet specific QoS criteria. For example, we propose a simple heuristic algorithm that finds an efficient configuration in terms of jitter, given an arbitrary throughput requirement (if such a configuration exists). Our method is detailed in Algorithm 1 and works as follows. It orders (by increasing order of values) the sets of possible values taken by d_0 and m in two sequences named $\mathcal{D}$ and $\mathcal{M}$, respectively. It then performs a binary search on $\mathcal{D}$: for a given d_0 in $\mathcal{D}$, it tests all combination
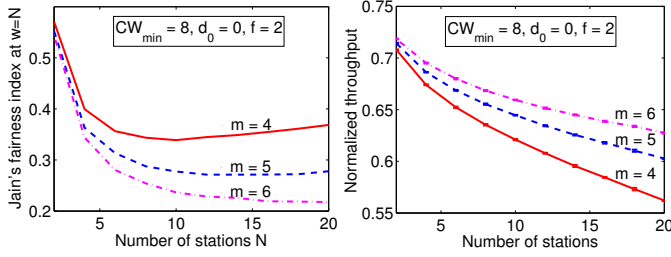
Fig. 12. Short-term fairness and throughput obtained by simulation with parameters $CW_{min} = 8, d_0 = 0, f = 2$ and various values of m.

	d_0		f		m		CW_{min}	
small	T ↗		T ↗		T ↘		T ↗ if N is small	
	F ↘		F ↘		F ↗		F →	
large	T ↘		T ↘		T ↗		T ↗ if N is large	
	F ↗		F ↗		F ↘		F →	

TABLE IV

SUMMARY OF THE QUALITATIVE EFFECTS OF EACH PARAMETER ON THROUGHPUT ("T") AND SHORT-TERM FAIRNESS ("F").

of parameters (m, CW_{min}) (by increasing order of m). When such a configuration satisfies the throughput requirement, the algorithm stores it and tries a larger value for d_0 (as a larger d_0 can potentially yield better jitter). Conversely, if no configuration meeting the throughput requirement is found, the algorithm considers smaller values for d_0 (which yield higher throughputs, potentially at the expense of jitter). The algorithm ends when it finds the best configuration that corresponds to the largest possible d_0 that satisfies the constraint.

Because it employs a binary search, the complexity of this algorithm is $O(|\mathcal{C}| \cdot |\mathcal{M}| \cdot \log(|\mathcal{D}|))$. We evaluate it on the sequences $\mathcal{C} = (8, 16, 32, 64)$, $\mathcal{M} = (4, 5, 6)$ and $\mathcal{D} = (0, 1, 2, 3)$[11]. First, we run simulations of all the possible configurations in $\{\mathcal{C} \times \mathcal{M} \times \mathcal{D}\}$, and we compute short-term fairness $J(N)$ and normalized throughput S. Let S_{min} be the minimum S achieved by all configurations in $\{\mathcal{C} \times \mathcal{M} \times \mathcal{D}\}$, and similarly S_{max} be the maximum S. To test our algorithm, we draw 100 throughput requirements uniformly at random in $[S_{min}, S_{max}]$. Then, for each sample i with throughput S_i, we run Algorithm 1 that returns the configuration $config_i$. Now, let J_i be the short-term fairness of the configuration $config_i$ at sample i, and let J_i^{max} denote the maximum short-term fairness of all configurations that satisfy the throughput constraint S_i. To evaluate the algorithm, we employ a normalized fairness index that is defined as J_i/J_i^{max}. The normalized fairness is a metric that evaluates the distance between the fairness of the configuration $config_i$ and the maximum achievable fairness given the the throughput constraint S_i.

The results of the algorithm evaluation are presented in Figure 13. We present the normalized fairness of the configurations returned from 100 runs of Algorithm 1. We repeat the procedure described above for $2 \leq N \leq 8$. We observe that Algorithm 1 always returns a configuration with good fairness given the throughput constraint. Thus, it can be employed

[11]We use the factor $f = 2$ because the contention windows are also doubled between successive backoff stages. Algorithm 1 can be modified to include different f values given the performance tradeoff of f in Table IV.
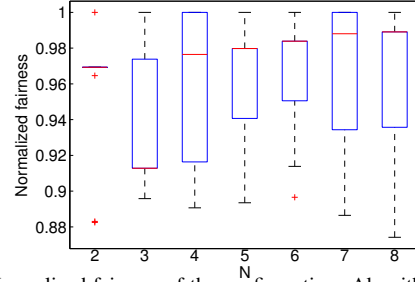

Fig. 13. Normalized fairness of the configurations Algorithm 1 returns when run for 100 throughput requirements S chosen randomly, for each N value.

to optimize the performance for delay-sensitive traffic that operates with 1901.

Algorithm 1: 1901 configuration for minimum jitter

1 **Input:** Throughput requirement S, number of stations N, sequences $\mathcal{D}$, $\mathcal{M}$ and $\mathcal{C}$ of possible values for d_0, m and CW_{min}, respectively
2 **Output:** A configuration (d_0, m, CW_{min}) that minimizes the jitter and provides throughput at least S, if it exists (returns `null` otherwise)
3 **Initialize:**
4 Sort the sequences $\mathcal{M}$ and $\mathcal{D}$ by increasing order of values
5 Set $h_1 \leftarrow 0$ and $h_2 \leftarrow |\mathcal{D}| - 1$
6 Set $config \leftarrow$ `null`

7 **while** $h_1 \leq h_2$ **do**
8   Set $break\_flag \leftarrow$ `false`
9     $h_3 \leftarrow \lceil (h_2 - h_1)/2 \rceil + h_1$
10   Set $d_0 \leftarrow \mathcal{D}_{h_3}$ (i.e., the h_3-th element of sequence $\mathcal{D}$)
11   **for** *each $m \in \mathcal{M}$ and $CW_{min} \in \mathcal{C}$* **do**
12   evaluate throughput $\hat{S}$ from model when using configuration (d_0, m, CW_{min})
13   **if** $\hat{S} \geq S$ **then**
14   Set $config \leftarrow (d_0, m, CW_{min})$
15   Set $h_1 \leftarrow h_3 + 1$
16   Set $break\_flag \leftarrow$ `true`
17   **break** out of **for** loop
18   **end**
19   **end**
20   **if** $break\_flag ==$ `false` **then**
21   Set $h_2 \leftarrow h_3 - 1$
22   **end**
23 **end**
24 **Return:** $config$

VII. CONCLUSION

The IEEE 1901 CSMA/CA protocol has received little attention from the research community so far, although it is adopted by the vast majority of power-line communication devices. In this paper, we focus on the analysis of the performance of this protocol. One of the key results is the finding that the decoupling assumption, which is commonly adopted for the analysis of MAC protocols such as IEEE 802.11 and IEEE 1901, might not hold for 1901. This is due to the coupling that this protocol introduces to the stations contending for the medium. Building on this finding, we have proposed a new model that does not rely on the decoupling assumption and thus substantially improves the accuracy of previous studies, in particular for networks with a small number of stations, the most frequent configuration in practice. Our model reveals that,

as a result of the coupling between stations, 1901 suffers from short-term unfairness. To address this issue, we have explored the tradeoff between short-term fairness and throughput that exists in 1901. In this context, we devised a method that computes efficient configurations in terms of fairness/jitter, under arbitrary throughput constraints.

APPENDIX

In this Appendix we give the proofs of some lemmas for Theorem 1. Table V can be used as a quick reference for the equations of Section IV.

Notation	Value	Eq.
x_k^i	$\sum_{j=d_i+1}^{k} \binom{k}{j} p_i^j (1-p_i)^{k-j}$	(2)
p_i	$1 - \frac{p_e}{1-\tau_i}$	(1)
p_e	$\prod_{k=0}^{m-1} (1-\tau_k)^{\bar{n}_k}$	-
bc_i	$\frac{\sum_{k=d_i+1}^{CW_i-1} \left[(k+1)(1-x_k) + \sum_{j=d_i+1}^{k} j(x_j - x_{j-1}) \right]}{CW_i}$ $+ \frac{(d_i+1)(d_i+2)}{2CW_i}$	(3)
τ_i	$\frac{\sum_{k=d_i+1}^{CW_i-1} \frac{1}{CW_i}(1-x_k) + \frac{d_i+1}{CW_i}}{bc_i}$	(4)
β_i	$\frac{\sum_{k=d_i+1}^{CW_i-1} \frac{1}{CW_i} \sum_{j=d_i+1}^{k} (x_j - x_{j-1})}{bc_i}$	(5)
K_i	$K_0 = 1, K_i = \frac{\tau_{i-1} p_{i-1} + \beta_{i-1}}{\tau_i + \beta_i}, 1 \le i \le m-2$ $K_{m-1} = \frac{\tau_{m-2} p_{m-2} + \beta_{m-2}}{\tau_{m-1}(1-p_{m-1})}$	(7)
$\bar{n}_i$	$\bar{n}_0 = \frac{N}{\sum_{k=0}^{m-1} \prod_{j=0}^{k} K_j}$, $\bar{n}_i = \frac{N \prod_{j=0}^{i} K_j}{\sum_{k=0}^{m-1} \prod_{j=0}^{k} K_j} 1 \le i \le m-1$	(EQ)

TABLE V
SUMMARY OF VARIABLES

Lemma 1. τ_i *is a decreasing function of p_i for any i.*

Proof. The probability τ_i given by (4) can be recast as

$$\tau_i = \frac{1}{B_i + 1} \quad (11)$$

where B_i is the expected number of backoff slots between two transmission attempts of a station that always stays at backoff stage i. B_i can be computed recursively and similarly to bc_i in (3), and it is given by[12]

$$B_i = \frac{d_i(d_i+1)}{2CW_i} \quad (12)$$
$$+ \sum_{j=d_i+1}^{CW_i-1} \frac{j(1-x_j) + \sum_{k=d_i+1}^{j} (k+B_i)(x_k - x_{k-1})}{CW_i}.$$

[12]From now on, we drop the superscript in x_k^i, because the backoff stage is clear from the context.

We simplify (12) as

$$B_i = \underbrace{\frac{d_i(d_i+1)}{2CW_i} + \sum_{j=d_i+1}^{CW_i-1} \frac{j}{CW_i}}_{1} - \underbrace{\sum_{j=d_i+1}^{CW_i-1} \frac{jx_j}{CW_i}}_{3}$$
$$+ \frac{1}{CW_i} \sum_{j=d_i+1}^{CW_i-1} \sum_{k=d_i+1}^{j} \left(\underbrace{B_i(x_k - x_{k-1})}_{2} + \underbrace{k(x_k - x_{k-1})}_{3} \right)$$
$$= \underbrace{\frac{CW_i-1}{2}}_{1} + \frac{1}{CW_i} \sum_{j=d_i+1}^{CW_i-1} \left(\underbrace{B_i x_j}_{2} - \underbrace{\sum_{k=d_i+1}^{j-1} x_k}_{3} \right), \quad (13)$$

where we have used that $x_{d_i} = 0$, for all $p_i \in [0,1]$ by the definition of x_k, and we have combined the terms with the same under-brace indexes.

To prove the lemma, we proceed as follows. (i) First, we compute dB_i/dp_i. (ii) Second, we show that this derivative is positive at $p_i = 1$. (iii) Third, we show that if the derivative is negative for some $0 < p_i^* < 1$, it will also be negative at any value $p_i > p_i^*$. The proof then follows by contradiction: if the derivative was negative at some p_i^*, it would also be negative at $p_i = 1$, which would contradict our previous result.

(i) The derivative of B_i can be computed as

$$\frac{dB_i}{dp_i} = \sum_{k=d_i+1}^{CW_i-1} \frac{\partial B_i}{\partial x_k} \frac{dx_k}{dp_i}. \quad (14)$$

The partial derivative $\partial B_i / \partial x_k$ can be computed by (13) as

$$\frac{\partial B_i}{\partial x_k} = \frac{B_i - (CW_i - 1 - k)}{CW_i} + \frac{\partial B_i}{\partial x_k} \sum_{j=d_i+1}^{CW_i-1} \frac{x_j}{CW_i}, \quad (15)$$

which yields

$$\frac{dB_i}{dp_i} = \frac{\sum_{k=d_i+1}^{CW_i-1} (B_i - (CW_i - 1 - k)) \frac{dx_k}{dp_i}}{CW_i - \sum_{j=d_i+1}^{CW_i-1} x_j}. \quad (16)$$

To compute dx_k/dp_i, we observe that x_k is the complementary cumulative function of a binomial distribution and it can be expressed as the incomplete beta function $x_k = 1 - I_{1-p_i}(k - d_i, d_i + 1)$ [17]. The derivative of an incomplete beta function is computed in [23], and by using this we obtain

$$\frac{dx_k}{dp_i} = \frac{k!}{(k - d_i - 1)! d_i!} p_i^{d_i} (1-p_i)^{k-d_i-1}. \quad (17)$$

(ii) Next, we show that $dB_i/dp_i > 0$ at $p_i = 1$. Note that $x_k = 1$ at $p_i = 1$ for all $d_i + 1 \le k \le CW_i - 1$. Given this, we have

$$B_i = \frac{d_i(d_i+1)}{2CW_i} + \frac{CW_i - d_i - 1}{CW_i}(d_i + 1 + B_i). \quad (18)$$

Solving (18) over B_i yields $B_i = CW_i - d_i/2 - 1$ at $p_i = 1$. Now, notice that $dx_k/dp_i = 0$ at $p_i = 1$ for all $d_i + 1 < k \le CW_i - 1$, and $dx_{d_i+1}/dp_i = d_i + 1$ from (17). Substituting in (16) yields $dB_i/dp_i = d_i/2 + 1$, i.e., $dB_i/dp_i > 0$ at $p_i = 1$.

(*iii*) Next, we show that if dB_i/dp_i was negative at some value p_i^*, then it would also be negative for any $p_i > p_i^*$. Observe that in (16) some terms are negative for $k < CW_i - 1 - B_i$. Let us assume that the derivative is negative at p_i^*. Let $l = \lceil CW_i - 1 - B_i(p_i^*) \rceil$. Given (16), we can express dB_i/dp_i as the product of two terms, $dB_i/dp_i = f_1(p_i)f_2(p_i)$, where

$$f_1(p_i) \doteq \frac{dx_l^i/dp_i}{CW_i - \sum_{j=d_i+1}^{CW_i-1} x_j^i},$$

$$f_2(p_i) \doteq \sum_{k=d_i+1}^{CW_i-1} (B_i - (CW_i - 1 - k))\frac{dx_k^i/dp_i}{dx_l^i/dp_i}.$$

Note that $f_1(p_i) > 0 \ \forall p_i$, which implies $dB_i/dp_i < 0$ if and only if $f_2(p_i) < 0$. Note also that

$$\frac{df_2(p_i)}{dp_i} = \sum_{k=d_i+1}^{CW_i-1} \frac{dB_i}{dp_i}\frac{dx_k^i/dp_i}{dx_l^i/dp_i} \qquad (19)$$
$$+ \sum_{k=d_i+1}^{l-1} (B_i - (CW_i - 1 - k))\frac{d}{dp_i}\left(\frac{dx_k^i/dp_i}{dx_l^i/dp_i}\right)$$
$$+ \sum_{k=l+1}^{CW_i-1} (B_i - (CW_i - 1 - k))\frac{d}{dp_i}\left(\frac{dx_k^i/dp_i}{dx_l^i/dp_i}\right)$$

and

$$\frac{d}{dp_i}\left(\frac{dx_k^i/dp_i}{dx_l^i/dp_i}\right) = -\frac{k!(l-d_i-1)!}{l!(k-d_i-1)!}(k-l)(1-p_i)^{k-l-1},$$

which is positive for $k < l$ and negative for $k > l$. From the above equations, it follows that as long as $CW_i - 1 - (l-1) > B_i(p_i) > CW_i - 1 - l$ and $dB_i/dp_i < 0$, we have $df_2/dp_i < 0$.

Building on the above, next we show that $B_i(p_i)$ decreases for $p_i \in [p_i^*, p_i^l]$, where p_i^l is the p_i value for which $B_i(p_i^l) - (CW_i - 1 - l) = 0$. At $p_i = p_i^*$ we have $f_2(p_i^*) < 0$, $dB_i/dp_i < 0$ and $df_2/dp_i < 0$. Let us assume that, before $B_i(p_i)$ decreases down to $CW_i - 1 - l$, there is some $\hat{p}_i > p_i^*$ for which $dB_i/dp_i \geq 0$. This implies that for some $p_i' \in (p_i^*, \hat{p}_i)$, $f_2(p_i)$ has to stop decreasing, i.e., $df_2(p_i')/dp_i = 0$. Note that, since $f_2(p_i)$ decreases in $[p_i^*, p_i']$, we have $f_2(p_i) < 0$ for $p_i \in [p_i^*, p_i']$, which implies that $B_i(p_i)$ decreases in $[p_i^*, p_i']$. Also, since $CW_i - 1 - (l-1) > B_i(p_i^*) > CW_i - 1 - l$ and (by assumption) $B_i(p_i)$ does not reach $CW_i - 1 - l$, we also have $CW_i - 1 - (l-1) > B_i(p_i') > CW_i - 1 - l$. However, we have seen that $f_2(p_i') < 0$ and $CW_i - 1 - (l-1) > B_i(p_i') > CW_i - 1 - l$ implies $df_2(p_i')/dp_i < 0$, which contradicts $df_2(p_i')/dp_i = 0$. Hence, our initial assumption does not hold, which implies that dB_i/dp_i decreases until B_i reaches $CW_i - 1 - l$, i.e., $dB_i/dp_i < 0$ for $p_i \in [p_i^*, p_i^l]$.

Following the same rationale for $p_i \in [p_i^l, p_i^{l+1}]$ and choosing

$$f_1(p_i) = \frac{dx_{l+1}^i/dp_i}{CW_i - \sum_{j=d_i+1}^{CW_i-1} x_j^i},$$

$$f_2(p_i) = \sum_{k=d_i+1}^{CW_i-1} (B_i - (CW_i - 1 - k))\frac{dx_k^i/dp_i}{dx_{l+1}^i/dp_i},$$

we can prove that $dB_i/dp_i < 0$ for $p_i \in [p_i^l, p_i^{l+1}]$. We can repeat this recursively to show that $dB_i/dp_i < 0$ for $p_i \in [p_i^{l+1}, p_i^{l+2}]$, $p_i \in [p_i^{l+2}, p_i^{l+3}]$ until reaching $p_i \in [p_i^{CW_i-2}, p_i^{CW_i-1}]$. If $1 < p_i^{CW_i-1}$, the proof is completed. Otherwise, we can follow a similar argument to show that $dB_i/dp_i < 0$ for $p_i \in [p_i^{CW_i-1}, 1]$. Indeed, let us assume that $f_2(p_i) \geq 0$ for some $\hat{p}_i \in [p_i^{CW_i-1}, 1]$. This implies that for some $p_i' \in [p_i^{CW_i-1}, \hat{p}_i]$, we have $df_2(p_i')/dp_i = 0$ and $f_2(p_i') < 0$, which is not possible according to (19).

From the above, if dB_i/dp_i was negative at any p_i^*, it would also be negative for all $p_i > p_i^*$. Since this contradicts result (*ii*), we conclude that $dB_i/dp_i \geq 0$ for $p_i \in [0, 1]$. $\qquad \square$

Corollary 1. τ_i *is a strictly decreasing sequence of i, and p_i is a strictly increasing sequence of i if $CW_{i+1} \geq 2CW_i - d_i - 1$, $0 \leq i < m - 1$.*

Proof. The result for τ_i follows from Lemma 1. By the proof of Lemma 1, the minimum value of B_{i+1} is $B_{i+1}^{min} = (CW_{i+1} - 1)/2$ at $p_{i+1} = 0$, and the maximum value of B_i is $B_i^{max} = CW_i - d_i/2 - 1$ at $p_i = 1$. Setting $CW_{i+1} \geq 2CW_i - d_i - 1$, yields $B_{i+1}^{min} \geq B_i^{max}$, hence $B_{i+1} > B_i$, and, as a result, $\tau_{i+1} < \tau_i$, for all $p_i \in [0, 1]$. From the above, p_i is strictly increasing with i because $p_i = 1 - p_e/(1 - \tau_i)$ and p_e is the same for all backoff stages i. $\qquad \square$

Corollary 2. β_i *is an increasing function of p_i.*

Proof. From (4) and (5), we have $\beta_i = 1/bc_i - \tau_i$. bc_i in (3) can be simplified as follows:

$$bc_i = \frac{CW_i + 1}{2} - \frac{\sum_{k=d_i+1}^{CW_i-1}\sum_{j=d_i+1}^{k} x_j}{CW_i}. \qquad (20)$$

Since $dx_k/dp_i > 0, k \geq d_i + 1$, bc_i is decreasing with p_i. Hence, by using Lemma 1, β_i is increasing with p_i. $\qquad \square$

Proposition 1. *Let us assume that τ_i is a strictly decreasing sequence of i. Then, according to the system of equations (1) for all $0 \leq i \leq m - 1$, p_e is defined in $[0, 1 - \tau_0^{max}]$, where τ_0^{max} is the maximum value of the transmission probability τ_0 at backoff stage 0.*

Proof. First, because of (1) and $p_i \leq 1$ for all $0 \leq i \leq m - 1$, we have that $p_e \geq 0$.

Now, because of (1) and $p_i \geq 0$, we have that $p_e \leq 1 - \tau_i$, for all τ_i values. From this, we have that p_e has to satisfy the condition $p_e \leq 1 - \tau_i^{max}$, where τ_i^{max} is the maximum value of τ_i, at $p_i = 0$. From the above and because τ_i is a strictly decreasing sequence of i (hence, we have $1 - \tau_i^{max} \geq 1 - \tau_0^{max}$), p_e has to satisfy $p_e \leq 1 - \tau_0^{max}$ in order to have $p_i \geq 0$, for all $0 \leq i \leq m - 1$. $\qquad \square$

Proposition 2. τ_i *can be expressed as an one-to-one function of p_e. All the relationships between τ_i, p_i, β_i and p_e are bijective.*

Proof. Let $\tau_0^{max} := 2/(CW_0 + 1)$ denote the maximum transmission probability at stage 0, which is equal to the transmission probability experienced by the only station in the channel when $N = 1$. According to Proposition 1, the

minimum and maximum values of p_e are 0 and $1 - \tau_0^{max}$, at $p_i = 1$, $0 \le i \le m - 1$ and $p_1 = 0$, respectively. We show that for each value $p_e \in [0, 1 - \tau_0^{max}]$ there exists a unique τ_i value, which results from combining (4) with (1). This implies that the function $\tau_i(p_e)$ resulting from combining (4) with (1) is one-to-one. The results for p_i, β_i then follow: For any value p_e, p_i can be computed given $\tau_i(p_e)$ and p_e by (1). Then, β_i is computed simply as a function of p_i using (5).

For any fixed value p_e^*, τ_i can be computed via the fixed-point equation

$$\tau_i = \frac{\sum_{k=d_i+1}^{CW_i-1} \frac{1}{CW_i}(1 - x_k(p_e^*, \tau_i)) + \frac{d_i+1}{CW_i}}{bc_i(p_e^*, \tau_i)} := f(p_e^*, \tau_i), \tag{21}$$

where we have replaced p_i with $1 - p_e^*/(1 - \tau_i)$ in the expressions for x_k (see (2)) and bc_i (see (3)). Because $f(p_e^*, \tau_i)$ maps the set of possible values of τ_i to itself, $f(p_e^*, \tau_i)$ has at least one fixed-point by Brouwer's fixed-point theorem. The solution to the above fixed-point equation is unique because the function $f(p_e^*, \tau_i)$ is continuous with respect to τ_i and strictly increasing:

$$\frac{df}{d\tau_i} = \frac{df}{dp_i}\frac{dp_i}{d\tau_i} = \frac{1}{(B_i + 1)^2}\frac{dB_i}{dp_i}\frac{p_e^*}{(1 - \tau_i)^2} > 0,$$

by using the proof of Lemma 5. Note that the above derivative might be 0 at $p_i = 0$ (when $d_i \ne 0$) due to $dB_i/dp_i = 0$, and it is also equal to 0 at $p_e^* = 0$. At these trivial values, it is easy to see that again, combining (4) with (1) yields a unique value for τ_i. Thus, (21) has a unique solution for any p_e^*, and $\tau_i(p_e)$ is an one-to-one function. It then follows by (1) that also the relationship between p_e and p_i is bijective. Now, given that β_i is monotone, hence one-to-one, with respect to p_i by Corollary 2, the relationship between p_e and β_i is also bijective. $\square$

Using the above proposition, we can express all variables τ_i, p_i, β_i as a function of p_e. The following lemma shows that $\tau_i(p_e)$ is an increasing function of p_e.

Lemma 2. *Let us consider the expression of τ_i as a function of p_e resulting from combining (4) with (1). According to this expression, τ_i is an increasing function of p_e, if $CW_i \ge 6$ and $d_i \le \lfloor CW_i/2 - 1 \rfloor$.*

Proof. Since $\tau_i = 1/(B_i + 1)$, we need to show that $dB_i/dp_e < 0$. Note that

$$\frac{dB_i}{dp_e} = \frac{dB_i}{dp_i}\frac{dp_i}{dp_e}. \tag{22}$$

From $p_i = 1 - p_e/(1 - \tau_i) = 1 - p_e(B_i + 1)/B_i$, we have

$$\frac{dp_i}{dp_e} = -\frac{B_i + 1}{B_i} + \frac{p_e}{B_i^2}\frac{dB_i}{dp_e}. \tag{23}$$

Combining (22) and (23) yields

$$\frac{dB_i}{dp_e} = -\frac{dB_i}{dp_i}\frac{B_i + 1}{B_i}\frac{1}{1 - \frac{p_e}{B_i^2}\frac{dB_i}{dp_i}}. \tag{24}$$

Because of Lemma 1, $dB_i/dp_i > 0$, and therefore $dB_i/dp_e < 0$ as long as

$$\frac{dB_i}{dp_i} < \frac{B_i^2}{p_e} = \frac{B_i(B_i + 1)}{1 - p_i}. \tag{25}$$

From (16) we have

$$\frac{dB_i}{dp_i} < \frac{B_i}{CW_i - \sum_{k=d_i+1}^{CW_i-1} x_k} \sum_{k=d_i+1}^{CW_i-1} \frac{dx_k}{dp_i}. \tag{26}$$

To prove the lemma, we distinguish two cases: one for $d_i = 0$ and one for $d_i \ne 0$.

First, let us study (26) with $d_i = 0$. We have $dx_k/dp_i = k(1 - p_i)^{k-1}$ and $x_k = 1 - (1 - p_i)^k$. Let $h(p_i) = \sum_{k=0}^{CW_i-1} k(1 - p_i)^k / \sum_{k=0}^{CW_i-1}(1 - p_i)^k$. We now show that h decreases with p_i. Let also $G(p_i) = \sum_{k=0}^{CW_i-1} p_i^k / \sum_{k=0}^{CW_i-1} kp_i^k$. By Lemma 5.1 in [11], $G(p_i)$ is strictly decreasing with p_i in $[0, 1]$. Thus, $h(p_i) = 1/G(1 - p_i)$ is also strictly decreasing with p_i in $[0, 1]$, and $h(p_i) \le h(0) = (CW_i - 1)/2$. Also, $B_i(p_i) \ge (CW_i - 1)/2$ by Lemma 1. Given the above, we have $h(p_i) \le B_i(p_i)$ and (26) yields

$$\frac{dB_i}{dp_i} < \frac{B_i}{1 - p_i}\frac{\sum_{k=0}^{CW_i-1} k(1 - p_i)^k}{\sum_{k=0}^{CW_i-1}(1 - p_i)^k} \le \frac{B_i^2}{1 - p_i} < \frac{B_i(B_i + 1)}{1 - p_i}.$$

We now move to the case $d_i \ne 0$. We show that $dB_i/dp_i < B_i^2$, which is a sufficient condition for (25). From (17) and (2) we have $dx_k/dp_i = k(x_k - x_{k-1})/p_i$. Thus, (26) yields

$$\frac{dB_i}{dp_i} < \frac{B_i}{p_i}\frac{CW_i x_{CW_i-1} - \sum_{k=d_i+1}^{CW_i-1} x_k}{CW_i - \sum_{k=d_i+1}^{CW_i-1} x_k} \le \frac{B_i}{p_i} x_{CW_i-1}.$$

Let $g(p_i) = B_i p_i - x_{CW_i-1}$. Now, it is sufficient to show that $g \ge 0$ for $p_i \in [0, 1]$ so that $x_{CW_i-1} \le B_i p_i$. Note that $g(0) = 0$, hence a sufficient condition now is $dg/dp_i > 0$. Let X be a random variable following the binomial distribution $\text{Bin}(CW_i - 2, p_i)$. Then, observe that using (17) we have

$$\frac{dg}{dp_i} = B_i + \frac{dB_i}{dp_i}p_i - (CW_i - 1)\mathbb{P}(X = d_i). \tag{27}$$

Since $B_i \ge (CW_i - 1)/2$ and dB_i/dp_i by Lemma 1, $dg/dp_i > 0$ if $\mathbb{P}(X = d_i) < 1/2$. The maximum of $\mathbb{P}(X = d_i)$ is at $p_i = d_i/(CW_i - 2)$. We show that $\mathbb{P}(Y = d_i) < 1/2$, where Y now is a random variable following the binomial distribution $\text{Bin}(CW_i - 2, d_i/(CW_i - 2))$. To this end, we use Theorem 2.1 in [24] that introduces some bounds on the binomial coefficient $\binom{n}{k}$. This theorem states that

$$\binom{n}{k} < \left(1 - \frac{5(k - 1)}{6n^2}\right)\frac{n(n - 1)^{n-1}}{k^k(n - k)^{n-k}} \tag{28}$$

for $n \ge 4$ and $2 \le k \le \lfloor n/2 \rfloor$. With $n = CW_i - 2$ and $k = d_i$, the above yields

$$\mathbb{P}(Y = d_i) < \left(1 - \frac{5(d_i - 1)}{6(CW_i - 2)^2}\right)\left(1 - \frac{1}{CW_i - 2}\right)^{CW_i-3}.$$

The above is smaller than 0.42 because $CW_i \ge 6$. Note that the above result holds for $d_i \ge 2$. For $d_i = 1$ we have

$$\mathbb{P}(Y = 1) = \left(1 - \frac{1}{CW_i - 2}\right)^{CW_i-3} = 0.42.$$

This completes the proof of the lemma. □

Let $\Phi(p_e) = \prod_{k=0}^{m-1} (1 - \tau_k(p_e))^{\bar{n}_k(p_e)}$. By using Proposition 2, we can express all $\beta_i(p_e)$, $p_i(p_e)$, $\tau_i(p_e)$, as a function of p_e. The following lemmas examine the function $\Phi(p_e)$ where each $\bar{n}_k(p_e)$ is a function of all $\beta_i(p_e)$, $p_i(p_e)$, $\tau_i(p_e)$, $0 \leq i \leq m - 1$ by (EQ).

Lemma 3. *Let* $\Phi(p_e) = \prod_{k=0}^{m-1} (1 - \tau_k(p_e))^{\bar{n}_k(p_e)}$, *where each* $\bar{n}_k(p_e)$ *is a function of all* $\beta_i(p_e)$, $p_i(p_e)$, $\tau_i(p_e)$, $0 \leq i \leq m - 1$. *Then,* $\partial\Phi/\partial\beta_j > 0$, *for any* $0 \leq j < m - 1$, *and* $\partial\Phi/\partial\beta_{m-1} = 0$, *if* $CW_{i+1} > 2CW_i - d_i - 1$, $0 \leq i \leq m - 1$.

Proof. We consider the expression $\prod_{k=0}^{m-1} (1 - \tau_k)^{\bar{n}_k}$ as a function of τ_i, p_i and β_i, where $\bar{n}_i$ is computed as a function of τ_i, β_i and p_i from (EQ). We show that if we increase β_j for a given j, and leave the remaining τ_i, p_i and β_i values fixed, then $\prod_{k=0}^{m-1} (1 - \tau_k)^{\bar{n}_k}$ increases. From (7), it can be seen that the new K_i values, denoted by K_i^*, satisfy the following.

If $j = 0$, then $K_1^* > K_1$ and $K_i^* = K_i$, $i > 1$ by (7). Thus, $\bar{n}_0^* < \bar{n}_0$ and $\bar{n}_i^* > \bar{n}_i$, $0 < i \leq m - 1$[13]. If $j = m - 1$, then $K_i^* = K_i$ and $\bar{n}_i^* = \bar{n}_i$, $0 \leq i \leq m - 1$, thus $\partial\Phi/\partial\beta_{m-1} = 0$.

Now, for $1 \leq j \leq m - 2$, we have $\prod_{n=1}^{i} K_n^* = \prod_{n=1}^{i} K_n$, $i < j$ and $\prod_{n=1}^{j} K_n^* < \prod_{n=1}^{j} K_n$.

We also have $\prod_{n=1}^{i} K_n^* > \prod_{n=1}^{i} K_n$, $i > j$, because

$$\frac{\prod_{n=1}^{i} K_n^*}{\prod_{n=1}^{i} K_n} = \frac{\frac{\tau_j p_j + \beta_j^*}{\tau_j + \beta_j^*}}{\frac{\tau_j p_j + \beta_j}{\tau_j + \beta_j}}, \quad \frac{\partial}{\partial\beta_j}\left(\frac{\tau_j p_j + \beta_j}{\tau_j + \beta_j}\right) = \frac{\tau_j(1 - p_j)}{(\tau_j + \beta_j)^2} > 0.$$

Let $\sigma = \sum_{i=1}^{m-1} \prod_{n=1}^{i} K_n$. We now show that $\sigma^* > \sigma$. We need to show that $\partial\sigma/\partial\beta_j > 0$. For $j = m - 2$, $\partial\sigma/\partial\beta_j > 0$ if and only if $\tau_{m-2}(1 - p_{m-2}) - \tau_{m-1}(1 - p_{m-1}) > 0$, which holds by Corollary 1. For $j < m - 2$, we prove $\sigma^* > \sigma$ by induction. We first show that $\sigma^* > \sigma$ for $j = m - 3$, and then prove that if it holds for $j = k$, then it holds for $j = k - 1$. Taking $\partial\sigma/\partial\beta_j$ we have

$$\partial\sigma/\partial\beta_j =$$

$$\prod_{l=1}^{j-1} \frac{K_l}{\tau_j + \beta_j}\left(-K_j + \frac{K_j\tau_j(1-p_j)}{\tau_{j+1} + \beta_{j+1}}\left(1 + \sum_{i=j+2}^{m-1}\prod_{n=j+2}^{i} K_n\right)\right)$$

Thus, we need to show that:

$$\tau_j(1 - p_j)\left(1 + \sum_{i=j+2}^{m-1}\prod_{n=j+2}^{i} K_n\right) - \tau_{i+1} - \beta_{i+1} > 0. \quad (29)$$

For $j = m - 3$, we have

$$\tau_{m-3}(1 - p_{m-3})(1 + K_{m-1}) - \tau_{m-2} - \beta_{m-2}$$

$$= \tau_{m-3}(1 - p_{m-3}) + \tau_{m-3}(1 - p_{m-3})\frac{\tau_{m-2}p_{m-2} + \beta_{m-2}}{\tau_{m-1}(1 - p_{m-1})}$$

$$- \tau_{m-2} - \beta_{m-2}$$

[13]Here and in following inequalities we use the fact that the function $y(x) = ax/(b + cx)$ with $a, b, c \in \mathbb{R}^+$ is increasing. Replacing x with the K_j that increases and a, b, c with products of K_i that remain constant yields the corresponding relations.

$$> \tau_{m-3}(1 - p_{m-3}) + \tau_{m-2}p_{m-2} - \tau_{m-2} > 0,$$

because of Corollary 1. Hence, (29) holds.

Now assume that $\sigma^* > \sigma$ for $j = k$. We show that $\sigma^* > \sigma$ holds also for $j = k - 1$. Let us study (29) for $j = k - 1$:

$$\tau_{k-1}(1 - p_{k-1})\left(1 + \sum_{i=k+1}^{m-1}\prod_{n=k+1}^{i} K_n\right) - \tau_k - \beta_k$$

$$> \tau_{k-1}(1 - p_{k-1})\left(1 + K_{k+1}\frac{\tau_{k+1} + \beta_{k+1}}{\tau_k(1 - p_k)}\right) - \tau_k - \beta_k > 0,$$

by using (29) for $j = k$, (7), and Corollary 1. This completes the induction proof for $\sigma^* > \sigma$.

Finally, given $\sigma^* > \sigma$ we have shown that $\bar{n}_i^* < \bar{n}_i$, $i \leq j$. Clearly, since $\bar{n}_i^* < \bar{n}_i$, $i \leq j$ (the number of stations at these backoff stages decreases) and $\sum_k \bar{n}_k^* = \sum_k \bar{n}_k = N$ (the total number of stations is always preserved), there must exist a backoff stage $l > j$ such that $\bar{n}_l^* > \bar{n}_l$ (the number of stations at this backoff increases). Since for $i \geq l + 1$, $\bar{n}_i = K_i\bar{n}_{i-1}$ with $K_i^* = K_i$, it holds $\bar{n}_i^* > \bar{n}_i$, $\forall i > l$. Thus,

$$\frac{\prod_{k=0}^{m-1} (1 - \tau_k)^{\bar{n}_k^*}}{\prod_{k=0}^{m-1} (1 - \tau_k)^{\bar{n}_k}} = \prod_{k<l} (1 - \tau_k)^{\bar{n}_k^* - \bar{n}_k}\prod_{k \geq l} (1 - \tau_k)^{\bar{n}_k^* - \bar{n}_k}$$

$$> (1 - \tau_{l-1})^{\sum_{k<l}\bar{n}_k^* - \bar{n}_k}(1 - \tau_l)^{\sum_{k \geq l}\bar{n}_k^* - \bar{n}_k}.$$

Since $\sum_k \bar{n}_k^* = \sum_k \bar{n}_k = N$ and $\tau_l < \tau_{l-1}$, the above is larger than 1, which proves the lemma for $0 \leq j \leq m - 2$. □

Lemma 4. *Let* $\Phi(p_e) = \prod_{k=0}^{m-1} (1 - \tau_k(p_e))^{\bar{n}_k(p_e)}$, *where each* $\bar{n}_k(p_e)$ *is a function of all* $\beta_i(p_e)$, $p_i(p_e)$, $\tau_i(p_e)$, $0 \leq i \leq m - 1$. *Then,* $\partial\Phi/\partial p_j > 0$, *for any* $0 \leq j \leq m - 1$, *if* $CW_{i+1} > 2CW_i - d_i - 1$, $0 \leq i \leq m - 1$.

Proof. The proof is similar to Lemma 3. It can be easily seen from (7) that if p_j increases to p_j^*, we have

$$\prod_{n=1}^{i} K_n^* = \prod_{n=1}^{i} K_n, \; i \leq j \quad \text{and} \quad \prod_{n=1}^{i} K_n^* > \prod_{n=1}^{i} K_n, \; i > j.$$

Note that the above holds for $0 \leq j \leq m - 2$. For $j = m - 1$ we have

$$\prod_{n=1}^{i} K_n^* = \prod_{n=1}^{i} K_n, \; i < m-1, \quad \prod_{n=1}^{i} K_n^* > \prod_{n=1}^{i} K_n, \; i = m-1.$$

Thus, as $\sigma^* > \sigma$ (with $\sigma = \sum_{i=1}^{m-1}\prod_{n=1}^{i} K_n$) also holds here, it is $\bar{n}_i^* < \bar{n}_i$ for $i \leq j$ and $\bar{n}_i^* > \bar{n}_i$ for $i > j$, with $0 \leq j \leq m - 2$. For $j = m - 1$ we have $\bar{n}_i^* < \bar{n}_i$ for $i < m - 1$ and $\bar{n}_i^* > \bar{n}_i$ for $i = m - 1$. Then, following the same reasoning as for the above lemma, it can be seen that $\prod_{k=0}^{m-1} (1 - \tau_k)^{\bar{n}_k^*} > \prod_{k=0}^{m-1} (1 - \tau_k)^{\bar{n}_k}$, which proves the lemma. □

Lemma 5. *Let* $\Phi(p_e) = \prod_{k=0}^{m-1} (1 - \tau_k(p_e))^{\bar{n}_k(p_e)}$, *where each* $\bar{n}_k(p_e)$ *is a function of all* $\beta_i(p_e)$, $p_i(p_e)$, $\tau_i(p_e)$, $0 \leq i \leq m - 1$. *Then,* $\partial\Phi/\partial\tau_j < 0$, *for any* $0 \leq j \leq m - 1$, *if* $CW_{i+1} > 2CW_i - d_i - 1$, $0 \leq i \leq m - 1$.

Proof. When τ_j increases to τ_j^{*}[14], $\prod_{n=1}^{i} K_n^* = \prod_{n=1}^{i} K_n$ for $i < j$, and $\prod_{n=1}^{i} K_n^* < \prod_{n=1}^{i} K_n$ for $i = j$. For $i > j$ we have

$$\prod_{n=1}^{i} K_n^* = \prod_{n=1}^{i} K_n \frac{\frac{\tau_j^* p_j + \beta_j}{\tau_j^* + \beta_j}}{\frac{\tau_j p_j + \beta_j}{\tau_j + \beta_j}}, \text{ and}$$

$$\frac{\partial}{\partial \tau_j}\left(\frac{\tau_j p_j + \beta_j}{\tau_j + \beta_j}\right) = -\frac{\beta_j(1 - p_j)}{(\tau_j + \beta_j)^2} < 0.$$

Thus, $\prod_{n=1}^{i} K_n^* < \prod_{n=1}^{i} K_n$ for $i \geq j$. These yield $\sigma^* < \sigma$, where $\sigma = \sum_{i=1}^{m-1} \prod_{n=1}^{i} K_n$. From the above, $\bar{n}_i^* > \bar{n}_i$ for $i < j$ and $\bar{n}_j^* < \bar{n}_j$, because $K_j^* < K_j$. We distinguish two cases for $i > j$. Suppose that $\bar{n}_i^* < \bar{n}_i$ for $i > j$. Then, following the same reasoning as for Lemma 3, it can be seen that $\prod_{k \neq j}(1 - \tau_k)^{\bar{n}_k}$ decreases:

$$\frac{\prod_{k \neq j}(1 - \tau_k)^{\bar{n}_k^*}}{\prod_{k \neq j}(1 - \tau_k)^{\bar{n}_k}} = \prod_{k < j}(1 - \tau_k)^{\bar{n}_k^* - \bar{n}_k} \prod_{k > j}(1 - \tau_k)^{\bar{n}_k^* - \bar{n}_k}$$

$$< (1 - \tau_{j-1})^{\sum_{k<j} \bar{n}_k^* - \bar{n}_k}(1 - \tau_{j-1})^{\sum_{k>j} \bar{n}_k^* - \bar{n}_k}$$

$$= (1 - \tau_{j-1})^{\bar{n}_j - \bar{n}_j^*} < 1, \text{ because } \bar{n}_j - \bar{n}_j^* > 0.$$

Suppose now that $\bar{n}_i^* > \bar{n}_i$ for $i > j$. Then, $\prod_{k \neq j}(1 - \tau_k)^{\bar{n}_k}$ decreases because it is a product of the positive decreasing functions $(1 - \tau_k)^{\bar{n}_k}$ with respect to $\bar{n}_k$[15]. If we show that $(1 - \tau_j)^{\bar{n}_j}$ also decreases, the lemma will be proven.

$$\frac{\partial(1 - \tau_j)^{\bar{n}_j}}{\partial \tau_j} = -\bar{n}_j(1 - \tau_j)^{\bar{n}_j - 1} + \ln(1 - \tau_j)\frac{\partial \bar{n}_j}{\partial \tau_j}(1 - \tau_j)^{\bar{n}_j}.$$

By computing the partial derivative of $\bar{n}_j = K_j \bar{n}_{j-1}$, we have

$$\frac{\partial \bar{n}_j}{\partial \tau_j} = -\frac{\bar{n}_j}{\tau_j + \beta_j} + \frac{\partial \bar{n}_{j-1}}{\partial \tau_j}K_j \geq -\frac{\bar{n}_j}{\tau_j + \beta_j} \geq -\frac{\bar{n}_j}{\tau_j},$$

because $\partial \bar{n}_{j-1}/\partial \tau_j > 0$ from (EQ).

Combining the two equations above yields

$$\frac{\partial(1 - \tau_j)^{\bar{n}_j}}{\partial \tau_j} \leq \frac{\bar{n}_j(1 - \tau_j)^{\bar{n}_j}}{\tau_j}\left(-\frac{\tau_j}{1 - \tau_j} - \ln(1 - \tau_j)\right).$$

Since $-x/(1 - x) < \ln(1 - x)$, it follows that the above is smaller than 0, which completes the proof of the lemma. $\square$

REFERENCES

[1] C. Vlachou, A. Banchs, J. Herzen, and P. Thiran, "On the MAC for Power-Line Communications: Modeling Assumptions and Performance Tradeoffs," in *IEEE International Conference on Network Protocols (ICNP)*, 2014.
[2] HomePlug Alliance (retrieved 4/2014). https://www.homeplug.org/news/pr/view?item_key=1baefc307e4d175c53568548371cb1142772f4ca.
[3] A. Schwager, "An Overview of the HomePlug AV2 Technology," *Journal of Electrical and Computer Engineering*, vol. 2013, 2013.
[4] HomePlug Alliance (retrieved 4/2014). http://www.homeplug.org/tech/whitepapers/Connected_Home_Summits_2013.pdf.
[5] "IEEE Standard for Broadband over Power Line Networks: Medium Access Control and Physical Layer Specifications," *IEEE Std 1901-2010*, pp. 1–1586, 2010.
[6] G. Bianchi, "Performance analysis of the IEEE 802.11 distributed coordination function," *Selected Areas in Communications, IEEE Journal on*, vol. 18, no. 3, pp. 535–547, 2000.
[7] M. Chung, M. Jung, T. Lee, and Y. Lee, "Performance analysis of Home-Plug 1.0 MAC with CSMA/CA," *Selected Areas in Communications, IEEE Journal on*, vol. 24, no. 7, pp. 1411–1420, 2006.
[8] C. Vlachou, A. Banchs, J. Herzen, and P. Thiran, "Performance Analysis of MAC for Power-line Communications," in *ACM Sigmetrics*, 2014.
[9] C. Cano and D. Malone, "On Efficiency and Validity of Previous Homeplug MAC Performance Analysis," *arXiv preprint arXiv:1401.6803*, 2014.
[10] C. Vlachou, J. Herzen, and P. Thiran, "Fairness of MAC protocols: IEEE 1901 vs. 802.11," in *Power Line Communications and Its Applications (ISPLC), 2013 17th IEEE International Symposium on*, 2013, pp. 58–63.
[11] A. Kumar, E. Altman, D. Miorandi, and M. Goyal, "New Insights From a Fixed-Point Analysis of Single Cell IEEE 802.11 WLANs," *Networking, IEEE/ACM Transactions on*, vol. 15, no. 3, pp. 588–601, june 2007.
[12] J.-w. Cho, J.-Y. Le Boudec, and Y. Jiang, "On the asymptotic validity of the decoupling assumption for analyzing 802.11 MAC protocol," *Information Theory, IEEE Transactions on*, vol. 58, no. 11, pp. 6879–6893, 2012.
[13] K. Huang, K. Duffy, and D. Malone, "On the Validity of IEEE 802.11 MAC Modeling Hypotheses," *Networking, IEEE/ACM Transactions on*, vol. 18, no. 6, pp. 1935–1948, 2010.
[14] G. Sharma, A. Ganesh, and P. Key, "Performance Analysis of Contention Based Medium Access Control Protocols," *Information Theory, IEEE Transactions on*, vol. 55, no. 4, pp. 1665 –1682, april 2009.
[15] G. Berger-Sabbatel, A. Duda, O. Gaudoin, M. Heusse, and F. Rousseau, "Fairness and its impact on delay in 802.11 networks," in *IEEE GLOBECOM '04*, vol. 5, nov.-3 dec. 2004, pp. 2967–2973 Vol.5.
[16] M. Bredel and M. Fidler, "Understanding Fairness and its Impact on Quality of Service in IEEE 802.11," in *INFOCOM 2009, IEEE*, pp. 1098 –1106.
[17] (2014) Binomial Distribution CDF. http://en.wikipedia.org/wiki/Binomial_distribution.
[18] (2014) Properties of Incomplete Beta Functions. http://functions.wolfram.com/GammaBetaErf/BetaRegularized/16/01/01/.
[19] C. Vlachou, J. Herzen, and P. Thiran. Simulator and Experimental Framework for the MAC of Power-Line Communications, Technical Report, 2014. documents.epfl.ch/users/v/vl/vlachou/www/1901_plc/experimental_framework.pdf.
[20] OpenWrt. http://https://openwrt.org/.
[21] Atheros Open Powerline Toolkit. https://github.com/qca/open-plc-utils.
[22] H. W. Jain R., Chiu D.M., "A quantitative measure of fairness and discrimination for resource allocation in shared computer systems," *DEC Research Report TR-301*, 1984.
[23] Wolfram. (2014) Incomplete Beta Function. http://functions.wolfram.com/GammaBetaErf/BetaRegularized/20/ShowAll.html.
[24] Z.-H. Sun. (2013) Inequalities for binomial coefficients. http://arxiv.org/abs/1310.0353.

---

[14]Note that due to Corollary 1, the sequence τ_i is still strictly decreasing with i, because the maximum value of τ_j is less than the minimum value of τ_{j-1}. Moreover, since we increase only τ_j, the inequality $\tau_j > \tau_{j+1}$ is preserved.

[15]The function $f(x) = a^x$ is decreasing if $a < 1$.